Separation of solutes with an organic solvent nanofiltration cascade: Designs, simulations and systematic study of all configurations

T. Renouard, A. Lejeune, M. Rabiller-Baudry

Separation of solutes with an organic solvent nanofiltration cascade: designs, simulations and systematic study of all configurations

Thierry Renouard*, Antoine Lejeune, Murielle Rabiller-Baudry

Université de Rennes 1, Université Bretagne Loire, UMR 6226 «Institut des Sciences Chimiques de Rennes» CNRS, 263 avenue du Général Leclerc, CS 74205, case 1011, 35042 Rennes cedex, France

*corresponding author: thierry.renouard@univ-rennes1.fr

Abstract

Due to the lack of efficient membranes to achieve subtle separations in a single step, membrane cascades appear as an alternative to improve the separation of solutes, especially in the case of close rejections. However, there is still a need for their rational design. In this work, a systematic study of all configurations up to seven stages is proposed through a unique and versatile simulation architecture. Different recycling modes in between stages are detailed and developed. The same VRR is imposed at each stage, ranging from 2 to 10. The case study is the olefin hydroformylation catalytic reaction, for which the simulations aim at the separation of two components, one modelling all organic products to extract in the permeate and the other one modelling the catalytic system to recover in the retentate for its further re-use in the synthesis reactor. Input data for the simulations (rejections and fluxes) are obtained from preliminary experimental studies. The separation performances are evaluated through seven criteria, amongst which the outflows extraction/recovery and the membrane area. The analysis of the simulation results allows to determine the optimal configuration that fulfills most of the targeted criteria or to fine tune these separation criteria according to the potentialities or the limitations of the membrane cascades. Even though focusing *a priori* on specific criteria, a careful attention should be paid to all parameters to ensure realistic proposals of cascades or to revise the objectives for more realistic ones.

Keywords

Organic solvent nanofiltration, membrane cascade, simulation, hydroformylation

1. Introduction

Organic solvent nanofiltration (OSN, alternatively named Solvent Resistant Nanofiltration - SRNF - or Organophilic Nanofiltration - ONF) is a technology of high potential of application in fine chemistry (*e.g.* for the recycling of homogeneous metal catalysts) [1–8], pharmaceutical industry [9,10] and petrochemistry [11,12]. Many lab-scale studies have led to promising results for the extraction of a target molecule or the recovery of a solvent [13,14]. However, for most of multicomponent media, the

available membranes are not enough selective to allow an effective separation in a single step. The compounds to retain are not fully recovered and those to extract are not completely transmitted resulting in a reciprocal contamination of the permeate and the retentate and in a weak overall quality of the two fractions with respect to their further use [6]. This moderate membrane performance is a drag to OSN industrial development and one of the reasons why few applications exist up to now [14,15].

A way to improve the separation of solutes is to use a membrane cascade. Such continuous process splits a feed stream into fractions either enriched or depleted in different components whose recovery and purity are controlled by the membrane materials, the operating conditions (hydrodynamics and concentrations) and the cascade design. Caus *et al.* [16] detailed the advantages of membrane cascades using the separation of xylose (150 $g.mol^{-1}$) and maltose (342 $g.mol^{-1}$) in water. First they measured the rejections with a single-stage set-up and then simulated cascades considering a constant rejection at each stage. The influence of the module volume recovery, the membrane characteristics and the number of stages (up to 4) in the cascade were assessed. The proof of concept at lab-scale for OSN was realized by Lin and Livingston [17] who experimentally performed a three-stage cascade with counter-current recycle for solvent exchange. Tetraoctylammonium was swapped from a 100% toluene solution to a 75.3% methanol solution thanks to the cascade. Siew *et al.* [18] combined simulation and experiments. They carried out a three-stage membrane cascade to concentrate an active pharmaceutical ingredient (API) in a mixture with 90% of ethyl acetate and 10% of methanol. The rejection was 55% with a single-stage set-up and increased up to 80% with a three-stage cascade. They reproduced by experiments the results of their simulation and succeeded to control the cascade showing the feasibility of this type of process for OSN applications in polar solvents.

Despite these relevant studies about membrane cascades, there is still a lack of methodology for their rational design that is currently made by a subsequent optimization. Abejón *et al.* [19] simulated OSN cascades up to 5 stages for the separation of an API from its impurity in methanol and optimized the process by a cost analysis dealing with pressure and recovery at each stage. Recently, Adi *et al.* [12] developed a superstructure membrane cascade for a crude oil refining application. The process improvement was oriented to increase the permeate purity but the extraction was only 5.5% of the overall mass of the feed stream. Moreover, numerical optimization made the importance of the cascade design difficult to appreciate because the influence of the optimization variables (transmembrane pressure and volume reduction ratio at each stage) was not assessed. Schmidt *et al.* [20] proposed a four-step design workflow integrating separation task analysis, solvent/membrane selection, experimental validation and process modelling. The case study was the recycling of a homogeneous rhodium catalyst represented by triphenylphosphine. The rejection of the triphenylphosphine was evaluated for cascades up to 5 stages with the possibility to add solvent at each stage. Rejections were ranging from 89.2% to +99.9%. Determination of the optimal design was established on the basis of

economic data to reduce the cost per ton of product.

This overview highlights a need of methodology for the rational design of membrane cascades but also to help end-users in the determination of realistic objectives based on the potentiality of membrane processes. In this study, systematic simulations of cascades up to seven stages are proposed. Different configurations and recycling modes are developed and explained. This allows to discuss the optimal configurations that fulfill targeted separation goals based on specific criteria.

2. Chemical reaction of interest

The approach detailed in this paper is of major interest when dealing with the post-treatment of organometallic catalyzed reaction media. In general, the final mixtures are characterized by a low concentration of any component from the catalytic system and a high concentration of the product with a product/catalyst ratio up to 100,000. The case study of this work is the homogeneous catalyzed hydroformylation of 10-undecenitrile to produce the linear aldehyde **A** in toluene (Fig. 1). The catalytic system is composed of a metal precursor and 20 equivalents of the Biphephos ligand **B**. In presence of a syngas (H_2/CO), an active catalyst **C** is obtained *in-situ* (1 metal center coordinated by 1 ligand **B**, 1 H atom and 1 molecule of carbon monoxide). This chemical reaction is of particular industrial interest since the linear aldehyde synthesized is a key intermediate for the preparation of Nylon-12. Even though several side-products are formed, for sake of simplification all simulations consider the post-treatment of a reaction with full conversion of the substrate and 100% selectivity for **A** (see section 4.1.1).

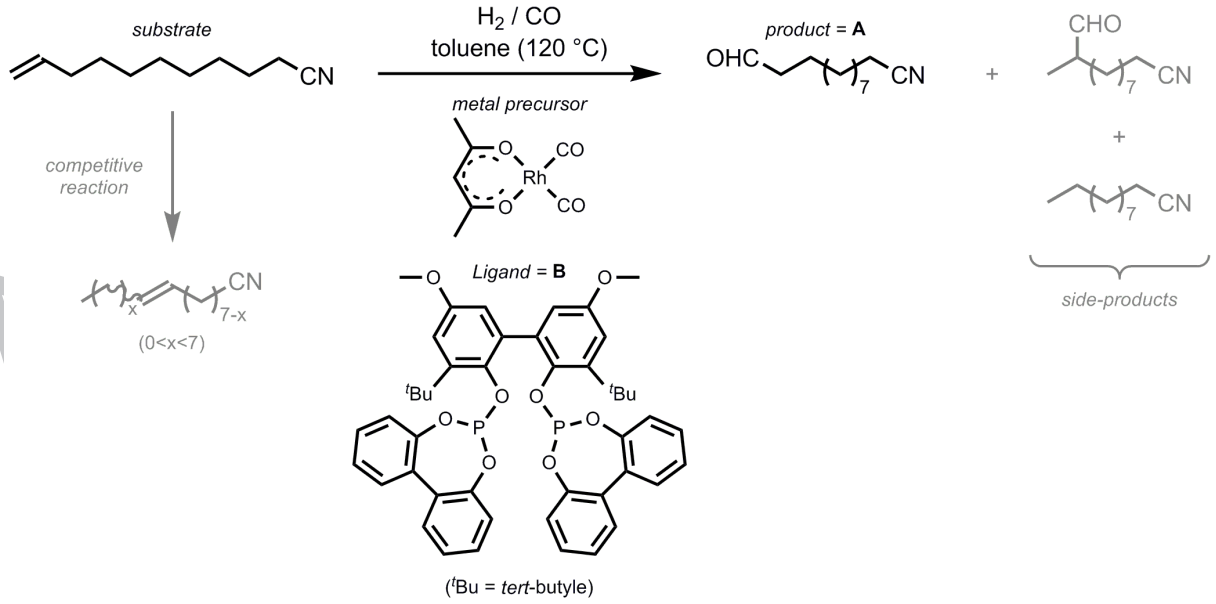

Figure 1: Hydroformylation catalytic reaction

The OSN objective is to extract the aldehyde **A** in the permeate and to recover the active catalyst **C**

and the extra free ligand **B** in the retentate so that they can be sent back to the reactor. General information about the components to separate is reported in Table 1.

Table 1: Hydroformylation final toluene mixture assuming full conversion and 100% selectivity for aldehyde A

	Aldehyde **A**	free Biphephos **B**	active Catalyst **C**
Molecular mass ($g.mol^{-1}$)	195	787	920
Ratio over metal precursor	20,000	19	1
Concentration at industrial scale ($mol.L^{-1}$)	1	$9.5 \cdot 10^{-4}$	$5 \cdot 10^{-5}$

It is worth noting that Rhodium is one of the most expensive noble metal and due to the ligand/metal ratio, ligand **B** accounts for approximately the same cost as the metal itself. Thus, the efficient recycling of the whole catalytic system is an economic challenge [20,21].

3. Theoretical approach of the design and modelling of membrane cascades

3.1. Design of membrane cascades

Membrane cascades are multistage processes where the mixture to filtrate passes through several membrane units. Different configurations can be *a priori* envisaged.

3.1.1. Basic configuration

In basic configuration, the membranes are connected "in series" (Fig. 2). Starting from a single-stage process (called stage *0*), one can add stages on the retentate side of stage *0* (labelled positively), add stages on the permeate side of stage *0* (labelled negatively), or both. Three sections are distinguished: (i) the feed stage (stage *0*) ; (ii) the retentate retreatment section (also called multistage [19,22] or stripping [18,23] section in reference to distillation) ; (iii) the permeate retreatment section (also called multipass [19,22] or enriching [18,23] section in reference to distillation). With such designs, the final retentate (respectively permeate) stream is the sum of the retentate (respectively permeate) outflow of the final stage of the corresponding retreatment section and all retentate (respectively permeate) outflows of the opposite section. Because of this mixing strategy, multicomponent mixtures coming from intermediate streams can pollute the final outflows which limits the separation efficiency [18] whereas without mixing high volumes are not recovered hence reducing the process interest. This type of design is already applied for reverse osmosis desalination processes [24] and will be further referred to as "no recycling". Pumps (not shown) are incorporated between stages to ensure the crossflow velocity and compensate the pressure drop. Recycling from one stage to another can be added to improve the separation performance of the cascades.

*3.1.2. Recycling "**-1**" configuration or counter-current recycle*

The most common type of recycling is the return of the "loss" fraction from one stage back to the feed of the previous one (namely the permeates in the retentate retreatment section and the retentates in the

permeate retreatment section) (Fig. 3a). This design will be further referred to as recycling "**-1**" and is also called counter-current recycle cascade [16,22,25].

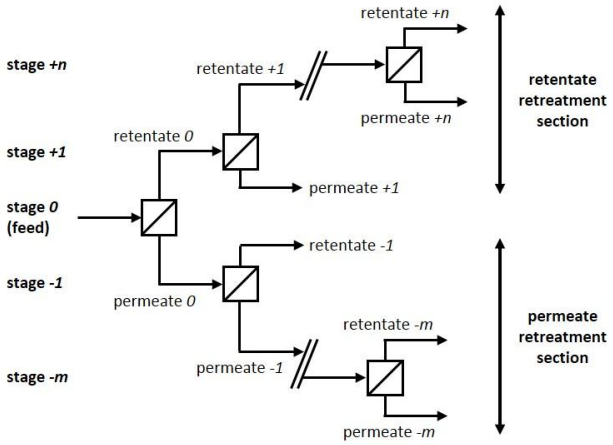

Figure 2: Basic configuration of membrane cascades ("no recycling")

For such membrane cascades with recycling between two consecutive stages, a comparison is possible with usual distillation processes where a plateau refers to a stage [26]. As in the case without recycling, the same three sections are defined in the cascade. Pumps are necessary for all recirculations and mixers (not shown) can be added to gather several streams. This configuration has only two outflows: one final retentate and one final permeate.

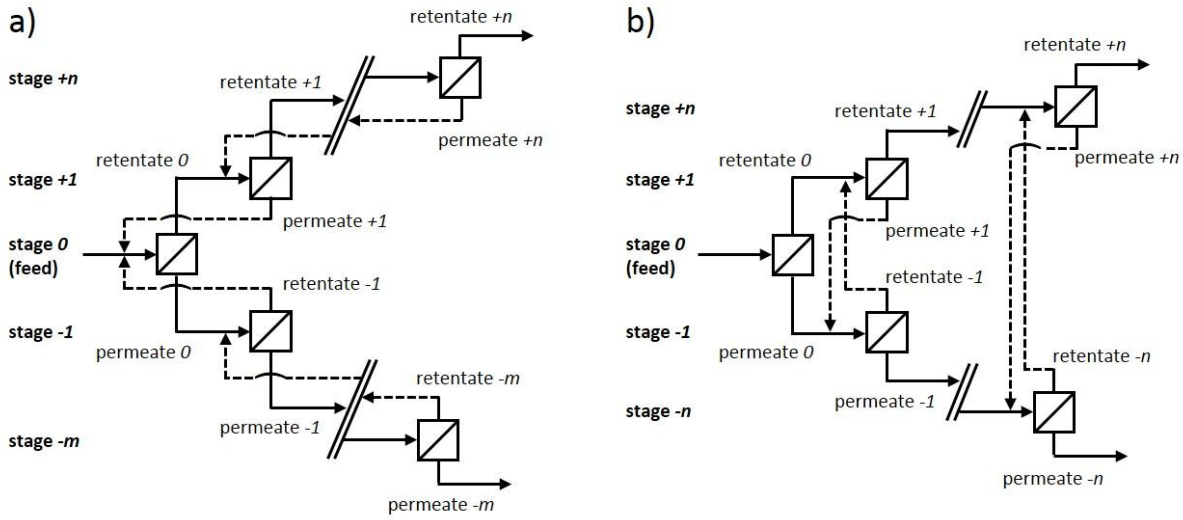

Figure 3: Membrane cascades with recycling (dashed lines) in both retreatment sections (a: recycling "-1" ; b: recycling "±")

3.1.3. Other recycling configurations

The recycling between stages can be different from recycling "**-1**". To discuss the interest of other types of recycling, based on the aforementioned cascade, two other designs are proposed. For the first one, all recycled streams are directed towards stage *0*. This design will be referred to as recycling "***→0***". This configuration requires a high membrane filtering area on stage *0* and is supposed to

increase the residence time of the solutes to separate in the membrane cascade aiming at an apparent and artificial increase of the number of stages.

For the second configuration, the recycled outflow from a stage is directed towards its counterpart in the opposite retreatment section (Fig. 3b) which imposes the same number of stages in both sections. This design will be referred to as recycling "±". Considering that any retentate is enriched in one solute compared to another one (and conversely for the permeate), the retentate retreatment section leads to a global enrichment in this solute (and conversely for the other solute in the permeate). Thus, the aim of this configuration is to drive any fraction enriched in one solute towards the corresponding enrichment section.

In the following, whatever the recycling mode, a systematic study is performed for all configurations up to seven stages. This limitation is probably too sophisticated/costly to be realistic for OSN applications except for products with very high value but allows to discuss a general approach enclosing the main possible applications.

3.2. Modelling of membrane cascades

3.2.1. Assumptions

Some assumptions are done to model the cascades: (i) continuous and steady-state process ; (ii) the feed of the membrane cascade is known (volumetric flowrate and concentrations or molar flowrates) ; (iii) a mixed outflow has homogeneous concentrations even if mixers are not indicated in the cascade ; (iv) a constant transmembrane pressure (TMP) is applied at any stage ; (v) the temperature is constant over the whole process.

3.2.2. OSN parameters

The notations used in the following equations are illustrated in Figure 4 and the definitions are presented in the Nomenclature part.

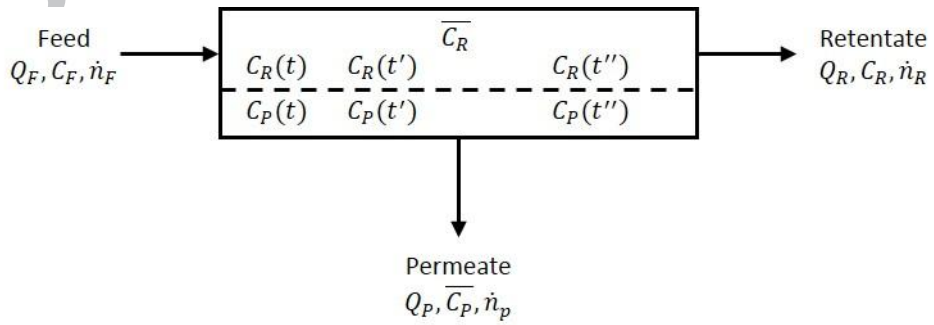

Figure 4: Outline of a membrane stage

Two process parameters have to be defined for the simulations. The first one is the rejection that is an experimental value and usually used as such over the whole cascade [6,25,27,28]. For our simulations, the rejection value needs to be estimated at each stage (see section 4.1.1). The rejection of a solute **X**

at stage *i* is given by Eq. 1.

$$R_{\mathrm{i}}(\mathbf{X})\ (\%) = \left(1 - \frac{\overline{C_{P,\mathrm{i}}}(\mathbf{X})}{\overline{C_{R,\mathrm{i}}}(\mathbf{X})}\right) \times 100 \quad (1)$$

With $\overline{C_{P,\mathrm{i}}}(\mathbf{X})$ (respectively $\overline{C_{R,\mathrm{i}}}(\mathbf{X})$) the permeate (respectively the retentate) average concentration of solute **X** at stage *i*. Note that the rejections are expressed as percentages, but values between 0 and 1 are used for the calculations.

The second parameter is the volume reduction ratio (VRR) that can be imposed either for each stage or for the whole cascade. In this study, for sake of simplification, the same VRR_i is applied to all stages:

$$VRR_{\mathrm{i}} = VRR = \frac{Q_{F,\mathrm{i}}}{Q_{R,\mathrm{i}}} \quad (2)$$

With $Q_{F,\mathrm{i}}$ the feed volumetric flowrate and $Q_{R,\mathrm{i}}$ the retentate volumetric flowrate at stage *i*.

Instead of VRR, the volume recovery (noted REC) is sometimes used [16,19,22]. This abbreviation may be ambiguous since REC can also represent the recovery of a solute (in mol%). Here we introduce the volume permeation ratio (VPR) that is defined by Eq. 3.

$$VPR_{\mathrm{i}} = VPR = \frac{Q_{P,\mathrm{i}}}{Q_{F,\mathrm{i}}} = 1 - \frac{1}{VRR} \quad (3)$$

With $Q_{P,\mathrm{i}}$ the permeate volumetric flowrate at stage *i*.

3.2.3. Mass balances for a single-stage process

For a single-stage process (noted stage *0*), unknown permeate and retentate variables (the volumetric flowrates and either the concentrations or the molar flowrates) have to be determined from the initial feed data. The two volumetric outflows are obtained using Eq. 2 and 3. For each solute, two additional equations are necessary. The first one is the solute mass balance that can be expressed using the molar flowrates:

$$\dot{n}_{F,0}(\mathbf{X}) = \dot{n}_{R,0}(\mathbf{X}) + \dot{n}_{P,0}(\mathbf{X}) \quad (4)$$

With $\dot{n}_{F,0}(\mathbf{X})$ the number of moles of solute **X** entering stage *0* per unit time and $\dot{n}_{R,0}(\mathbf{X})$ (respectively $\dot{n}_{P,0}(\mathbf{X})$) the number of moles of solute **X** in the retentate (respectively the permeate) leaving that stage per unit time.

The second equation is obtained by considering the evolution of the retentate concentration along the membrane module being divided into small elements (see appendix A). This equation is derived from the mathematical development of the abatment [29]:

$$\dot{n}_{R,0}(\mathbf{X}) = \dot{n}_{F,0}(\mathbf{X}) \times VRR^{[R_0(\mathbf{X})-1]} \quad (5)$$

3.2.4. Mass balances for a membrane cascade with recycling

Figure 5 represents three-stage membrane cascades with recycling and with 1 stage in each retreatment section. These configurations are chosen as examples of the modelling procedures for multistage processes.

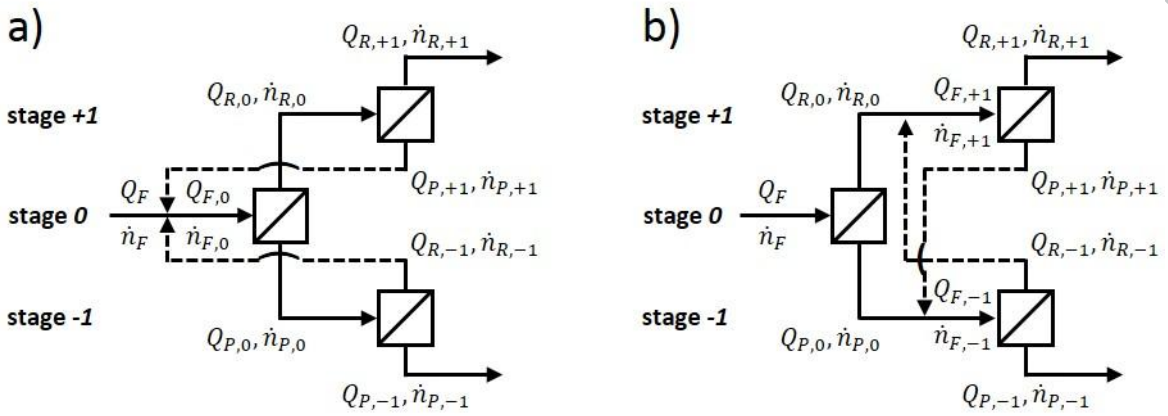

Figure 5: Unknown variables for three-stage membrane cascades with recycling (a: "-1" b: "±")

Each stage of the cascade can be modelled by the same 4 equations (Eq. 2-5) as for a single-stage process, giving a set of 12 equations. For recycling "**-1**", 14 unknown variables have to be determined for 1 solute. The last 2 equations necessary for the simulations are obtained by considering the mixing step leading to the actual feed of stage *0* [19,22]:

$$Q_{F,0} = Q_F + Q_{R,-1} + Q_{P,+1} \quad (6)$$

$$\dot{n}_{F,0} = \dot{n}_F + \dot{n}_{R,-1} + \dot{n}_{P,+1} \quad (7)$$

The same development can be drawn for recycling "**→*0***", but for recycling "±", 16 unknown variables have to be determined for 1 solute. In addition to the set of 12 equations, the last 4 equations correspond to the new feed streams for stages *+1* and *-1*:

$$Q_{F,+1} = Q_{R,0} + Q_{R,-1} \quad (8)$$

$$\dot{n}_{F,+1} = \dot{n}_{R,0} + \dot{n}_{R,-1} \quad (9)$$

And

$$Q_{F,-1} = Q_{P,0} + Q_{P,+1} \quad (10)$$

$$\dot{n}_{F,-1} = \dot{n}_{P,0} + \dot{n}_{P,+1} \quad (11)$$

4. Experimental

The experimental part concerns both nanofiltration results on which simulations are based and detailed information on the calculations.

4.1. OSN experimental data

4.1.1. Rejections

Some experimental data are requested prior to the simulations. Hydroformylation reaction mixtures are obtained starting from an initial substrate concentration of 1 mol.L^{-1} and with respect to the molecular ratios reported in Table 1. Nanofiltration of the solutions are performed on a Evonik-MET CrossFlow system at a transmembrane pressure (TMP) of 10 bar, up to VRR 2 and using a PDMS membrane (17 cm^2 area). The aldehyde **A** rejection (determined by GC analysis) and the ligand **B** rejection (determined by UV-Vis analysis) are 30% and 88% respectively. Note that the un-reacted substrate and all side-products have lower rejections than the target aldehyde **A** which favors their extraction (data not shown). The same way, the rejection of the active catalyst **C** is slightly higher than the rejection of ligand **B** which favors its recovery. Thus, considering only **A** (with a feed concentration of 1 mol.L^{-1}) for all organic products and **B** for simulating the whole catalytic system is the most difficult separation to perform.

Due to the high concentration of aldehyde **A** in the feed stream, the influence of this concentration on its rejection has been considered. A constant rejection of 30% is confirmed for concentrations below 1 mol.L^{-1}; but for higher concentrations, the experiments reveal a rejection decrease with the increase of the concentration, leading to the following equation to be applied to the cascade:

$$R_{\mathrm{i}}(\mathbf{A})\ (\%) = -3.4869 \times \overline{C_{R,\mathrm{i}}}(\mathbf{A})^2 + 3.6482 \times \overline{C_{R,\mathrm{i}}}(\mathbf{A}) + 29.738 \quad (12)$$

With $\overline{C_{R,\mathrm{i}}}(\mathbf{A})$ the retentate average concentration of aldehyde **A** at stage *i* that is calculated by:

$$\overline{C_{R,\mathrm{i}}}(\mathbf{A}) = \frac{\overline{C_{P,\mathrm{i}}}(\mathbf{A})}{1 - R_{\mathrm{i}}(\mathbf{A})} \quad (13)$$

With $\overline{C_{P,\mathrm{i}}}(\mathbf{A})$ the permeate average concentration of aldehyde **A** at stage *i* calculated thanks to $\dot{n}_{P,\mathrm{i}}(\mathbf{A})$ and $Q_{P,\mathrm{i}}$.

Since the rejection and both the permeate and the retentate average concentrations of aldehyde **A** are interdependent in Eq. 12 and 13, an iterative progress has to be performed for the simulations until convergence of the results: at start, the rejection is fixed at 30%, which allows to determine $\dot{n}_{P,\mathrm{i}}(\mathbf{A})$ (thanks to Eq. 4 and 5) leading to both average concentrations as mentioned above. The retentate average concentration is then applied in Eq. 12 to determine a new rejection value that is further used to recalculate $\dot{n}_{P,\mathrm{i}}(\mathbf{A})$ leading to new values for both average concentrations and so on until convergence of the rejection used and the one estimated.

The concentration of aldehyde **A** being 3 orders of magnitude that of ligand **B**, its influence on the rejection of ligand **B** has also been assessed leading to Eq. 14.

$$R_{\mathrm{i}}(\mathbf{B})\ (\%) = 0.0025 \times \overline{C_{R,\mathrm{i}}}(\mathbf{A})^2 - 2.0126 \times \overline{C_{R,\mathrm{i}}}(\mathbf{A}) + 90.01 \quad (14)$$

4.1.2. Permeate fluxes

In order to calculate the membrane filtering area needed at each stage, the permeance has been experimentally measured at TMP of 10 bar. Assuming that aldehyde **A** imposes the permeate flux due to its higher concentration than ligand **B**, several solutions ranging from 0 mol.L^{-1} (pure solvent) to 4.6 mol.L^{-1} (pure liquid solute **A**) have been filtrated leading to the following equations:

$$L_{P,\mathrm{i}} = 0.178 \times \overline{C_{R,\mathrm{i}}}(\mathbf{A})^2 - 0.996 \times \overline{C_{R,\mathrm{i}}} + 2.934 \quad \text{if } \overline{C_{R,\mathrm{i}}}(\mathbf{A}) < 2.5 \text{ mol.L}^{-1}$$

$$L_{P,\mathrm{i}} = -0.1 \times \overline{C_{R,\mathrm{i}}}(\mathbf{A}) + 1.8 \quad \text{if } \overline{C_{R,\mathrm{i}}}(\mathbf{A}) > 2.5 \text{ mol.L}^{-1} \quad (15)$$

4.2. Scope of the simulations and calculation details

4.2.1. Scope

The overall amount of aldehyde **A** to treat is 10,000 tons per year (Q_F = 6,400 L.h^{-1}) which corresponds to a medium scale industrial production. More than 75 different configurations of membrane cascades have been simulated varying the number of stages in each retreatment section and the presence of recycling. VRR 2, 4, 6, 8 and 10 are used for the simulations. The same VRR is imposed at each stage of the cascade to facilitate the understanding of the influence of the cascade design on the separation performances. The use of a different VRR per stage can be performed to optimize the process but is outside the scope of this study.

4.2.2. Calculations

All simulations are realized using a Microsoft Excel file. A unique architecture has been developed that gathers the "no recycling" mode and both recycling "**-1**" and "**→*0***" modes as illustrated in Figure 6. This architecture allows to simulate cascades up to 11 stages and to systematically evaluate all configurations up to 7 stages with at least one stage in both retreatment section, the feed stage being at any position. A different layout is established for recycling "±" due to its specificity. The aim of the calculations is to express a feed stage according to the feed of the previous one and its process parameters (*i.e.* the rejection and the VRR). In this work, any stage outflow is entirely redirected. Note that the possibility to split redirected outflows in several streams has also been considered when preparing the architecture (not shown). For example, the permeate of stage *+5* can be partly directed towards the final permeate stream of the cascade and partly recycled, with the possibility to partly direct the recycled stream towards any of the stages from *+4* to *0*.

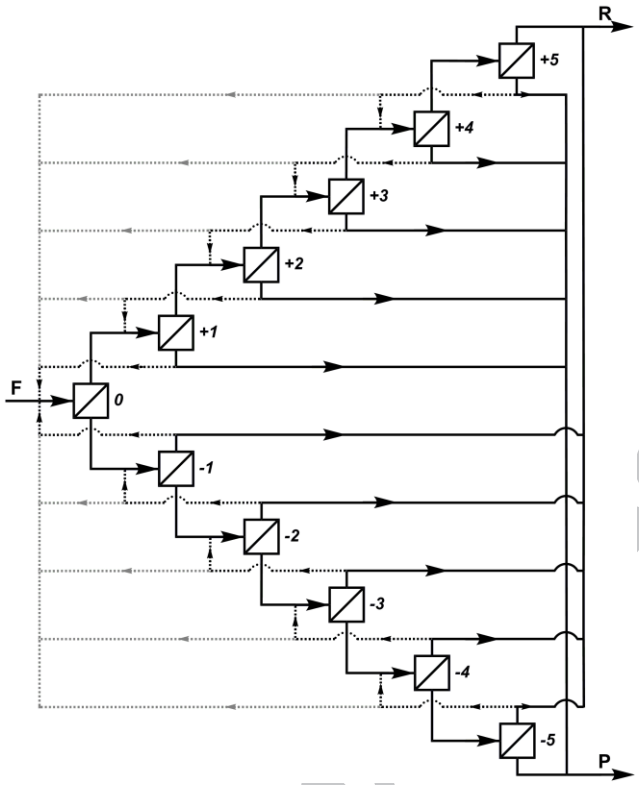

Figure 6: Outline of the unique simulation architecture combining "no recycling" (full lines), recycling "-1" (black dotted lines) and recycling "→*0*" (grey dotted lines)

The calculations developed in the Microsoft Excel file are examplified hereafter for one solute with recycling "**-1**". Except for the final stages, each feed stage in the retentate (respectively the permeate) retreatment section is the sum of two streams: the retentate (respectively the permeate) outflow of the previous stage and the permeate (respectively the retentate) outflow of the following stage. This direct addition can be applied to the volumetric flowrates (as usually developed for cascade simulations with recycling) but also to the molar flowrates, which ensures a useful simplification of the calculations compared to the use of the concentrations. For a better understanding of the strategy, the example starts from the final stage *+5*. According to Eq. 5:

$$\dot{n}_{F,+5} = \dot{n}_{R,+4} = \dot{n}_{F,+4} \times VRR^{(R_{+4}-1)} \tag{16}$$

Eq. 16 can also be expressed as:

$$\dot{n}_{F,+5} = \dot{n}_{F,+4} \times \frac{\alpha_{R,+4}}{1-\beta_{R,+5}} \tag{17}$$

With $\alpha_{R,\mathrm{i}} = VRR^{(R_\mathrm{i}-1)}$ for any stage *i* and $\beta_{R,+5} = 0$ (*vide infra*).

For stage *+4* and according to Eq. 4 and 5:

$$\dot{n}_{F,+4} = \dot{n}_{R,+3} + \dot{n}_{P,+5} = \dot{n}_{F,+3} \times \alpha_{R,+3} + \dot{n}_{F,+5} \times \alpha_{P,+5} \tag{18}$$

With $\alpha_{P,\mathrm{i}} = 1 - VRR^{(R_\mathrm{i}-1)} = 1 - \alpha_{R,\mathrm{i}}$ for any stage *i*.

By transposition of Eq. 17 in Eq. 18, the feed of stage *+4* can be expressed from the feed of stage *+3*:

$$\dot{n}_{F,+4} = \dot{n}_{F,+3} \times \frac{\alpha_{R,+3}}{1-\beta_{R,+4}} \quad (19)$$

With $\beta_{R,+4} = \frac{\alpha_{R,+4} \times \alpha_{P,+5}}{1-\beta_{R,+5}}$

Thus, for any stage *i* in the retentate retreatment section, the feed molar flowrate can be expressed from the feed molar flowrate of the previous stage according to the following equation:

$$\dot{n}_{F,\mathrm{i}} = \dot{n}_{F,\mathrm{i}-1} \times \frac{\alpha_{R,\mathrm{i}-1}}{1-\beta_{R,\mathrm{i}}} \quad (20)$$

With $\beta_{R,\mathrm{i}} = \frac{\alpha_{R,\mathrm{i}} \times \alpha_{P,\mathrm{i}+1}}{1-\beta_{R,\mathrm{i}+1}}$ and $\beta_{R,+\mathrm{n}} = 0$ for the final stage *+n*.

The same development can be done for any stage *j* (algebraic value) in the permeate retreatment section, which gives:

$$\dot{n}_{F,\mathrm{j}} = \dot{n}_{F,\mathrm{j}+1} \times \frac{\alpha_{P,\mathrm{j}+1}}{1-\beta_{P,\mathrm{j}}} \quad (21)$$

With $\beta_{P,\mathrm{j}} = \frac{\alpha_{P,\mathrm{j}} \times \alpha_{R,\mathrm{j}-1}}{1-\beta_{P,\mathrm{j}-1}}$ and $\beta_{P,-\mathrm{m}} = 0$ for the final stage *-m*.

For stage *0*:

$$\dot{n}_{F,0} = \dot{n}_F + \dot{n}_{R,-1} + \dot{n}_{P,+1} = \dot{n}_F + \dot{n}_{F,-1} \times \alpha_{R,-1} + \dot{n}_{F,+1} \times \alpha_{P,+1} \quad (22)$$

Which leads to:

$$\dot{n}_{F,0} = \frac{\dot{n}_F}{1-\beta_{P,0}-\beta_{R,0}} \quad (23)$$

4.2.3. Criteria to quantify the membrane cascade performances

Seven criteria are used to compare the performances of the various simulated membrane cascades.

• The extraction of aldehyde **A** in the final permeate stream:

$$Extraction\ of\ \mathbf{A}\ (\%) = \left(\frac{\dot{n}_P(\mathbf{A})}{\dot{n}_F(\mathbf{A})}\right) \times 100 \quad (24)$$

• The aldehyde **A** purity in the final permeate stream:

$$Purity\ of\ \mathbf{A}\ (\%) = \left(\frac{\dot{n}_P(\mathbf{A})}{\dot{n}_P(\mathbf{A}) + \dot{n}_P(\mathbf{B})}\right) \times 100 \quad (25)$$

• The recovery of ligand **B** in the final retentate stream:

$$Recovery\ of\ \mathbf{B}\ (\%) = \left(\frac{\dot{n}_R(\mathbf{B})}{\dot{n}_F(\mathbf{B})}\right) \times 100 \quad (26)$$

• The ligand **B** enrichment ratio in the final retentate stream is defined by Eq. 27. This is another way to deal with purity but the enrichment is more adapted here because ligand **B** is much less concentrated than aldehyde **A** and its purity is very low:

$$Enrichment\ of\ \mathbf{B} = \frac{\dot{n}_R(\mathbf{B})/\left(\dot{n}_R(\mathbf{A})+\dot{n}_R(\mathbf{B})\right)}{\dot{n}_F(\mathbf{B})/\left(\dot{n}_F(\mathbf{A})+\dot{n}_F(\mathbf{B})\right)} \quad (27)$$

• The overall membrane filtering area = sum of the membrane area at each stage:

$$A_{mb}\ (m^2) = \sum_{\mathrm{i}} \frac{Q_{P,\mathrm{i}}}{L_{P,\mathrm{i}} \times TMP} \quad (28)$$

With $L_{P,\mathrm{i}}$ being calculated according to Eq. 15.

• The global VRR of the cascade:

$$Global\ VRR = \frac{Q_F}{Q_R} \quad (29)$$

With Q_F the feed flowrate of the cascade and Q_R the final retentate flowrate of the cascade (Fig. 6).

• The energy consumption (all streams are considered, except the final retentate and permeate):

$$Q_{OSN}\ (kW) = \sum_{\mathrm{i}} \frac{TMP \times Q_{F,\mathrm{i}}}{\eta_{pump}} \quad (30)$$

With η_{pump} the pump efficiency equal to 0.7 from literature data [10].

5. Results and discussion

5.1. First approach of the cascades: Influence of the recycling mode and the VRR

Some preliminary simulations are realized in order to highlight the impact of the recycling mode and the VRR on the cascades performance and justify their specific selection for further detailed studies.

5.1.1. Influence of the recycling mode

The four different modes ("no recycling" and recycling "**-1**", "**→*0***" and "**±**") have been compared at VRR 2 at each stage. Due to the specificity of recycling "**±**", all configurations are composed of the same number of stages in both retreatment sections. Consequently cascades with odd numbers of stages from 3 to 11 are performed, although a number of stages higher than 7 should not be relevant for products with low added value. For the configuration with 3 stages, no data is reported for the recycling "**→*0***" since this is an equivalent recycling to the more general "**-1**".

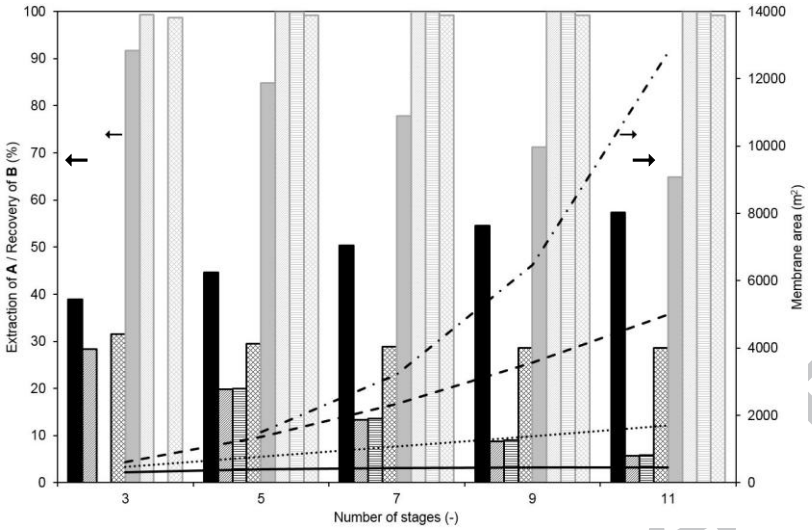

Figure 7: Impact of the recycling mode and the number of stages on the performances of the cascades (VRR 2 ; black: extraction of A ; grey: recovery of B ; solid bars and full line: "no recycling" ; obliques and dashed line: recycling "-1" ; horizontals and dash/dotted line: recycling "→*0*" ; crosses and dotted line: recycling "±")

The performances of the configurations are evaluated in terms of extraction of **A** in the permeate, recovery of **B** in the retentate and the overall membrane area needed to achieve the separation (Fig. 7).

For the design without recycling, the extraction of **A** slightly increases from 39% with 3 stages to 57% with 11 stages. In parallel, the recovery of **B** drops from 92% to 65%. This too poor recovery makes the "no recycling" configuration inadequate for industrial purposes.

All configurations with recycling reach at least 98% recovery of **B** whatever the number of stages, highlighting the interest to add a recycling for solutes with relatively high rejections. The results are more contrasted for the extraction of **A** and always quite low:

- The recycling "**→*0***" gives the same extraction of **A** than the recycling "**-1**" that regularly decreases from 28% with 3 stages to 6% with 11 stages. Nevertheless, it must be noted that even though similar extractions are reported for both configurations, the membrane area is much higher for the former recycling that needs an oversizing of the first stage.
- The configurations with recycling "±" present an original behavior since the extraction of **A** is almost constant (*ca.* 30%) whatever the number of stages and always higher than those obtained with the 2 other recycled configurations. In addition the membrane area is the lowest amongst all the recycling modes. However, this trend is not confirmed for VRR > 2. In fact, as soon as VRR 3, the extraction of **A** and the recovery of **B** are lower with recycling "±" compared to the 2 other recycling modes (not shown). Recycling "±" will not be further studied.

5.1.2. Influence of the VRR

Since our objective is to simulate the post-treatment of an industrial production thanks to OSN, VRR 2 appears insufficient and is not presented in the following. Figure 8 shows the simulated extraction of **A** and recovery of **B** thanks to several simple cascades with recycling "**-1**" and either a retentate

retreatment section or a permeate retreatment section. Each dot represents the combined results for 1 cascade design at a given VRR. The further from stage *0*, the more stages are added in the considered retreatment section. For example, the dot labelled (*+1 0*) corresponds to a two-stage cascade composed of 1 stage in the retentate retreatment section and the feed stage, whereas the dot labelled (*0 -1*) corresponds to a two-stage cascade composed of the feed stage and 1 stage in the permeate retreatment section, and so on.

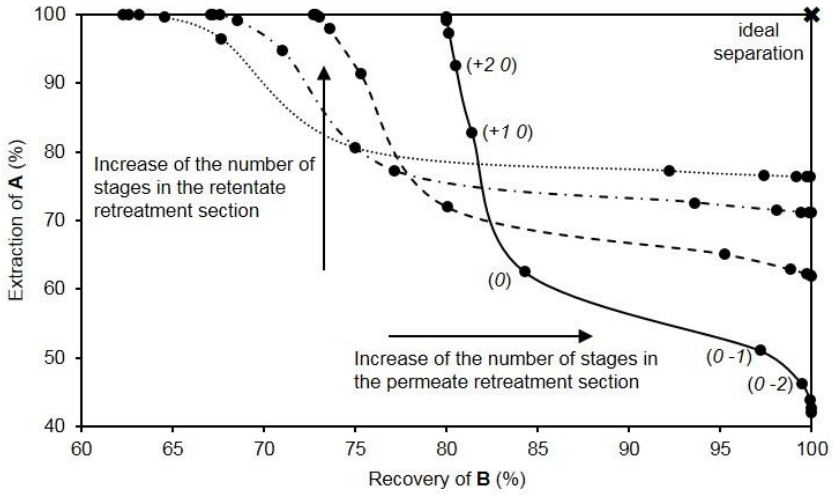

Figure 8: Performances of membrane cascades with recycling "-1" either in the retentate or in the permeate retreatment section (VRR at each stage: full line= 4 ; dashed line= 6 ; dash/dotted line= 8 ; dotted line= 10)

Increasing the number of stages in the retentate retreatment section allows to increase the extraction of **A** in the permeate but systematically decreases the recovery of **B** the in the retentate. An opposite trend is observed for the permeate retreatment section. In addition, whatever the number of stages and the retreatment section, the higher the VRR at each stage, the higher is the aldehyde **A** extraction but the lower is the ligand **B** recovery. This figure clearly shows that dealing with only one retreatment section (either permeate or retentate) do not allow to reach the "ideal separation" (100% of aldehyde **A** extraction and 100% of ligand **B** recovery) and so both retreatment sections have to be considered simultaneously in more sophisticated cascades.

5.2. Systematic simulation of sophisticated cascades with recycling "-1"

The goal is to determine the optimal membrane cascade design thanks to simulations that highlight the influence of the cascade configuration and the operating conditions (especially the VRR at each stage) on the separation performances. To be consistent with the previous part, recycling "**-1**" is selected as a representative configuration.

Figure 9 displays the results of the simulations performed at VRR 4. Starting from the single-stage process (*0*), the dashed lines represent simulations of the "no recycling" cascade and the full lines represent the same design with recycling "**-1**" highlighting that the "ideal separation" cannot be reached by incorporating stages in only one retreatment section. The addition of a stage in the retentate

retreatment section from the configuration (*0 -1*) or a stage in the permeate retreatment section from the configuration (*+1 0*) results in the same configuration corresponding to the dot (*+1 -1*). Thus, these 3 configurations are linked by dotted lines. As stated before, while increasing the number of stages in the retentate retreatment section, the extraction of **A** in the permeate increases but the recovery of **B** in the retentate decreases and conversely for the addition of stages in the permeate retreatment section. Increasing the number of stages in both sections tends towards the "ideal separation" objective. However, it has to be noted that the more additional stages, the shorter is the performance increase between 2 linked configurations, whatever the retreatment section. All these curves make an original mapping (as illustrated by the insert of Fig. 9) that can be used to determine which configuration (number of stages, feed stage position, recycling mode) and which VRR should be applied to reach a targeted separation goal.

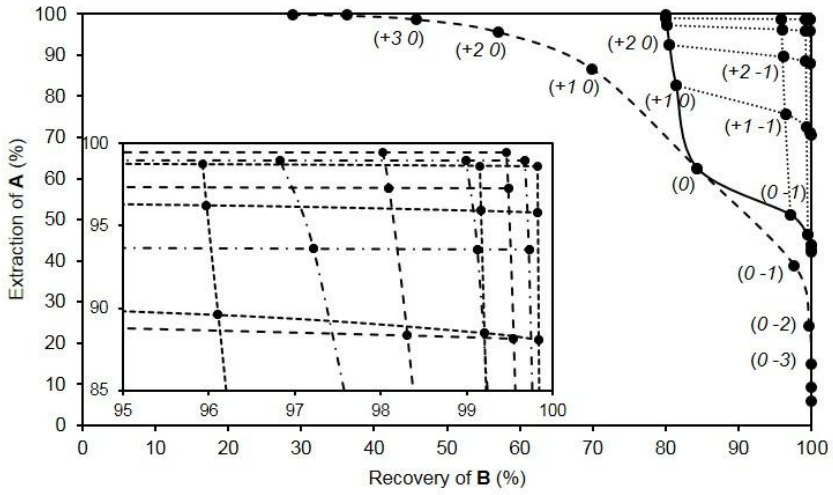

Figure 9: Performances of sophisticated cascades (VRR 4 at each stage) – dashed line: "no recycling" ; full line: recycling "-1" either in the retentate or in the permeate retreatment section ; dotted line: recycling "-1" in both retreatment sections. Insert: Mapping with VRR 4 (dotted line), VRR 6 (dashed line) and VRR 8 (dash/dotted line)

Optimization of a cascade is not only dealing with an efficient separation and high percentages of solutes in both outflow streams. The membrane filtering area is an important parameter to consider due to the membrane turnover (governed by the lifetime in the OSN conditions) and the energy needed for pumping. Figure 10 combines the results of figure 9 (mind the axes) with the overall membrane area of the different configurations. It is interesting to note that an efficient separation and a good solute recovery are not necessarily associated to the highest membrane areas. Similar performances are reached either by a five-stage cascade (*+3 -1*) or by a seven-stage cascade (*+3 -3*) but the membrane area is doubled for the latter. The membrane area is also related to the position of the feed stage in the cascade, since addition of stages in the retentate retreatment section will deal with reduced volumes due to VRR although addition of stages in the permeate retreatment section will deal with substantial volumes. For a global overview of all configurations, the same analysis has to be realized for all recycling modes and each VRR tested.

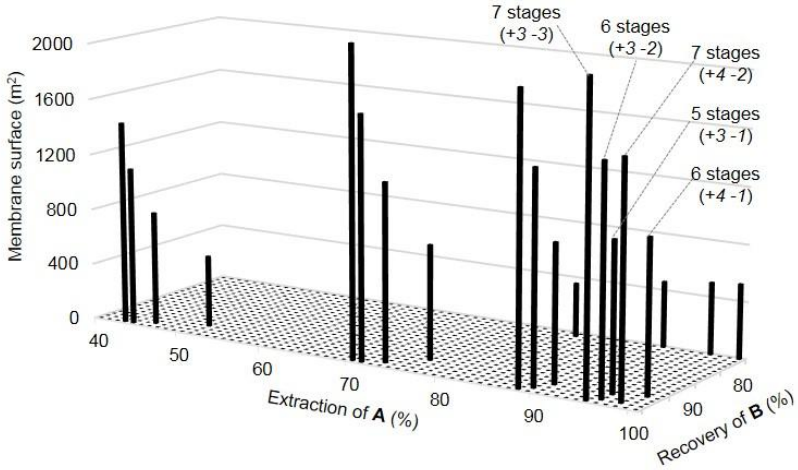

Figure 10: Membrane area *vs* separation performances for different configurations of cascades with recycling "-1" (VRR 4 at each stage)

5.3. Case studies depending on the objectives of the OSN treatment

For the industrial application targeted in this study, the efficient recycling of the whole catalytic system is crucial because of the cost of both rhodium and the free ligand **B** used in excess to run properly the reaction. The first objective is set at 99% recovery of **B**. A substantial extraction of the synthesized aldehyde **A** has to be envisaged. Two proposals are tested for the extraction of **A** from high requirement (95% extraction) to moderate requirement (80% extraction).

*5.3.1. Case study 1: 99% recovery of **B** and 95% extraction of **A***

By reaching that separation with a membrane cascade, OSN can be proposed as a unique purification step to replace the energy-consuming distillation process. No cascade design with less than 6 stages is able to perform such separation (Fig. 11a). Six different configurations of six-stage cascades fulfills the separation criteria, two of them with recycling "***→0***". The results are reported in table 2. The extraction of **A** ranges from 95.9% to 99.0% with an excellent purity observed for all configurations due to the huge concentration difference of **A** compared to **B**. The recovery of **B** is almost unchanged, but its enrichment depends on the VRR at each stage with more than a two-fold increase by changing the VRR from 6 to 8 for configuration (*+2 -3*), whatever the recycling mode. The position of the feed stage *0* in the configuration is of importance for the overall membrane area and (associated to the configuration) for the global VRR of the cascade. The more stages in the permeate retreatment section, the more is the membrane area in accordance with larger volumes to treat. In that way, configuration (*+1 -4*) has the larger membrane area (with recycling "**-1**") and needs the highest VRR at each stage. It is interesting to note that similar results are obtained with configurations (*+1 -4*) and (*+3 -2*) except for the membrane area, meaning that the position of the feed stage *0* may have an impact on the global cost of the cascade without altering its performance. As already stated (see section 5.1.1), recycling "***→0***" always leads to comparable extraction of **A** and recovery of **B** but to a larger membrane area compared to recycling "**-1**".

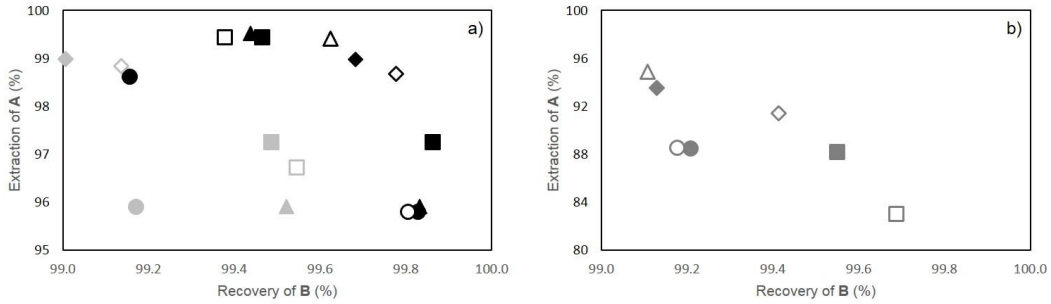

Figure 11: Outline of the configurations allowing 99% recovery of B and: a) 95% extraction of A ; b) 80% extraction of A (black: 7-stage ; light grey: 6-stage ; grey: 5-stage ; solid symbol: recycling "-1" ; empty symbol: recycling "→*0*" ; VRR: ● = 4 ;■ = 6 ; ◆ = 8 ; ▲ = 10 ; Note that the results of a) are omitted in b) for clarity)

The last two columns of Table 2 deal with the same configuration, but constant rejections for **A** and **B** were used for the latter. In that case, a slightly lower extraction of **A** parallel to a lower enrichment of **B** are observed. This is consistent with the fact that for the case where the rejections vary, the simulation imposes lower rejections for **A** and **B** when the concentration of **A** increases. It seems that variation of the rejections has only a poor impact on the simulation results. However, no consideration of this variation would have led to the exclusion of one possible configuration since the extraction of **A** appears below 95%. Moreover, it has to be pointed out that the final retentate concentration of **A** is 3.4 mol.L^{-1} when the rejections are not fixed and 9.3 mol.L^{-1} when constant rejections are used, which is physically impossible since the pure aldehyde **A** has a maximal concentration of 4.6 mol.L^{-1}.

Table 2: Results of the simulations with 95% extraction of A and 99% recovery of B for six-stage cascade designs

Configuration	(*+1 -4*)	(*+2 -3*)				(*+3 -2*)	(*+3 -2*)*
VRR at each stage	10	6		8		4	*4*
Recycling mode	-1	-1	→*0*	-1	→*0*	-1	*-1*
Extraction of **A** (%)	95.9	97.3	96.7	99.0	98.8	95.9	*88.9*
Purity of **A** (%)	>99.9	>99.9	>99.9	>99.9	>99.9	>99.9	*>99.9*
Recovery of **B** (%)	99.5	99.5	99.5	99.0	99.1	99.2	*99.4*
Enrichment of **B** (-)	23.8	35.2	29.5	88.9	78.9	23.7	*8.9*
Membrane area (m^2)	1927	1758	2067	1641	1859	1590	*1606*
Global VRR	81	125	105	343	301	84	*84*
Q_{OSN} (kW)	15.6	15.0	17.2	13.5	14.9	14.8	*14.8*

* Simulations with constant rejections (30% for **A** and 88% for **B**)

This clearly emphasizes that the criteria used to quantify the cascade performances have to be carefully selected and all parameters have to be checked. Amongst all results reported in Table 2, configuration (*+3 -2*) fulfills at minima the separation criteria with the lowest membrane area and configuration (*+2 -3*) with VRR 8 at each stage and recycling "**-1**" presents the best separation performances (highest recoveries and purities for **A** and **B**) associated to one of the lowest membrane area. However, for this latter configuration, the global VRR (>340) may not be realistic at industrial scale since it corresponds to a volumetric flowrate reduction from 6,400 L.h^{-1} for the feed stream to less than 19 L.h^{-1} for the final retentate, likely difficult to reach due to the hold-up volume of an

industrial equipment.

*5.3.2. Case study 2: 99% recovery of **B** and 80% extraction of **A** compatible with a limited global VRR*

For that case, the cascade should be considered as the first post-treatment step with 2 objectives. Firstly, since OSN is performed at room temperature, the catalytic system integrity is preserved which may allow its recycling. Secondly, due to the splitting of the feed stream into 2 fractions, the volume being further treated by distillation is reduced, which can have a significant impact on the energy saving and the cost of the global purification step. Considering the remark dealing with the reachable global VRR, the minimal separation goal was set at 80% extraction of **A** and 99% recovery of **B**. This reduction of the extraction goal of **A** allows to reduce the number of stages of the cascade. Seven new configurations of five-stage cascades fulfill the separation criteria, the majority of them being with recycling "***→0***" (Fig. 11b). Table 3 details the simulation results for these new configurations.

Table 3: Results of the simulations with 99% recovery of B and 80% extraction of A for five-stage cascade designs

Configuration	(*+1 -3*)					(*+2 -2*)	
VRR at each stage	6		8		10	4	
Recycling mode	-1	*→0*	-1	*→0*	*→0*	-1	*→0*
Extraction of **A** (%)	88.2	83.0	93.6	91.4	94.9	88.5	88.5
Purity of **A** (%)	>99.9	>99.9	>99.9	>99.9	>99.9	>99.9	>99.9
Recovery of **B** (%)	99.6	99.7	99.1	99.4	99.1	99.2	99.2
Enrichment of **B** (-)	8.4	5.8	15.2	11.5	19.0	8.6	8.6
Membrane area (m^2)	1639	1897	1577	1779	1700	1489	1617
Global VRR	25	18	49	39	67	28	28
Q_{OSN} (kW)	14.3	16.3	13.1	14.5	13.5	14.2	15.3

The same trends as previously observed can be drawn. The objective of reduction of the permeate volume makes the global VRR criterion of importance. In that sense, the recycling "***→0***" appears as promising since similar extractions/recoveries and purities are reached compared to recycling "**-1**" with a lower global VRR. A better selection of the optimal configuration can be based on the membrane area or the energy consumption criteria and by considering the added value of the product. Configuration (*+1 -3*) with VRR 8 at each stage and recycling "***→0***" associates a good extraction/recovery with a moderate global VRR and a limited membrane area.

Conclusion

In this paper, original equations for the simulation of cascades are developed. This allows to settle a flexible simulation architecture that gathers up to eleven stages and different recycling modes. Recycled streams are considered between consecutive stages, sent back to the feed stage or directed towards the opposite retreatment section. More than 75 different cascade configurations have been

systematically studied, each one being developed with several VRR ranging from 2 to 10. Graphical representations of the separation performances permit to select the best configuration based on specific criteria. A case study is aiming at the "catalytic system/reaction products" separation in a toluene mixture issued from the homogeneous catalyzed hydroformylation reaction. An ambitious separation goal (99% recovery of the catalytic system and 95% extraction of the products) reveals the (physical/cost) limitations of both the cascade designs and the simulation results. Indeed, only focusing on separation criteria can lead to excessive VRR and unreachable concentrations in the final streams. Optimization of the cascade simulations can be done by considering a variable VRR from one stage to another or by introducing other innovative recycling modes.

Acknowledgements

The authors thank the french ANR for the financial support of the project MemChem n° 14-CE06-0022 and the french clusters IAR and Axelera for labelling this project.

Prof. J.-F. Carpentier and L. Le Goanvic, Université de Rennes 1, are gratefully acknowledged for providing substantial amounts of hydroformylation reaction mixtures. The authors would like to thank Prof. D. Wolbert, ENS Chimie Rennes, for helpful discussions.

Nomenclature

A_{mb}	Membrane filtering area (m²)
$C_F(\mathbf{X})$	Feed concentration of solute **X** for the cascade (mol.L^{-1})
$C_{F,i}(\mathbf{X})$	Feed concentration of solute **X** at stage *i* (mol.L^{-1})
$C_{P,i}(\mathbf{X})$	Permeate concentration of solute **X** at stage *i* (mol.L^{-1})
$\overline{C_{P,i}}(\mathbf{X})$	Permeate average concentration of solute **X** at stage *i* (mol.L^{-1})
$C_{R,i}(\mathbf{X})$	Retentate concentration of solute **X** at stage *i* (mol.L^{-1})
$\overline{C_{R,i}}(\mathbf{X})$	Retentate average concentration of solute **X** at stage *i* (mol.L^{-1})
$L_{P,i}$	Membrane permeance at stage *i* (L.m^{-2}.h^{-1}.bar^{-1})
$\dot{n}_F(\mathbf{X})$	number of moles of solute **X** in the feed of the cascade (mol.h^{-1})
$\dot{n}_{F,i}(\mathbf{X})$	number of moles of solute **X** in the feed of stage *i* (mol.h^{-1})
$\dot{n}_{P,i}(\mathbf{X})$	number of moles of solute **X** in the permeate of stage *i* (mol.h^{-1})
$\dot{n}_{R,i}(\mathbf{X})$	number of moles of solute **X** in the retentate of stage *i* (mol.h^{-1})
Q_F	Feed flowrate of the cascade (L.h^{-1})
$Q_{F,i}$	Feed flowrate at stage *i* (L.h^{-1})
Q_{OSN}	Pumping energy (kW)
$Q_{P,i}$	Permeate flowrate at stage *i* (L.h^{-1})
$Q_{R,i}$	Retentate flowrate at stage *i* (L.h^{-1})

$R_i(\mathbf{X})$	Rejection of solute **X** at stage *i* (%)
TMP	Transmembrane pressure (bar)
VPR_i	Volume permeation ratio of stage *i* (-)
VRR_i	Volume reduction ratio of stage *i* (-)
η_{pump}	Pump efficiency (-)

Appendix A

In a steady-state flow and for one solute, 2 mass balance equations can be written:

Solvent mass balance:

$$Q_F = Q_P + Q_R \quad \text{(A.1)}$$

Solute mass balance:

$$Q_F \times C_F = Q_P \times C_P + Q_R \times C_R \quad \text{(A.2)}$$

Considering the 2 above equations and using the VPR (Eq. 3), one gets:

$$C_R = \frac{C_F - VPR \times C_P}{1 - VPR} \quad \text{(A.3)}$$

A nanofiltration module can be divided into an infinite number of small elements (Fig. A.1). In a small element starting from the module feed until a volume permeation ratio equal to vpr, Eq. A.3 becomes:

$$C'_R = \frac{C_F - vpr \times C'_P}{1 - vpr} \quad \text{(A.4)}$$

With $C_F < C'_R < C_R$.

The permeate concentration can also be calculated incorporating the rejection *R* (Eq. 1):

$$C'_P = \frac{1}{vpr} \times \int C'_P \times \mathrm{d}vpr = \frac{1}{vpr} \times \int (1 - R) \times C'_R \times \mathrm{d}vpr \quad \text{(A.5)}$$

Eq. A.4 and A.5 give:

$$C'_R = \frac{1}{1 - vpr} \times [C_F - \int (1 - R) \times C'_R \times \mathrm{d}vpr] \quad \text{(A.6)}$$

After derivation of Eq. A.6 according to vpr, one gets:

$$\frac{\mathrm{d}[C'_R \times (1 - vpr)]}{\mathrm{d}vpr} = \frac{\mathrm{d}C_F}{\mathrm{d}vpr} - (1 - R) \times C'_R \quad \text{(A.7)}$$

The derivation can also be expressed by Eq. A.8.

$$\frac{\mathrm{d}[C'_R \times (1 - vpr)]}{\mathrm{d}vpr} = (1 - vpr) \times \frac{\mathrm{d}C'_R}{\mathrm{d}vpr} + C'_R \times \frac{\mathrm{d}(1 - vpr)}{\mathrm{d}vpr} = (1 - vpr) \times \frac{\mathrm{d}C'_R}{\mathrm{d}vpr} - C'_R \quad \text{(A.8)}$$

In Eq. A.7, $\frac{\mathrm{d}C_F}{\mathrm{d}vpr} = 0$, hence combining Eq. A.7 and A.8 leads to:

$$\frac{\mathrm{d}C_R'}{\mathrm{d}vpr} = \frac{R \times C_R'}{1 - vpr} \tag{A.9}$$

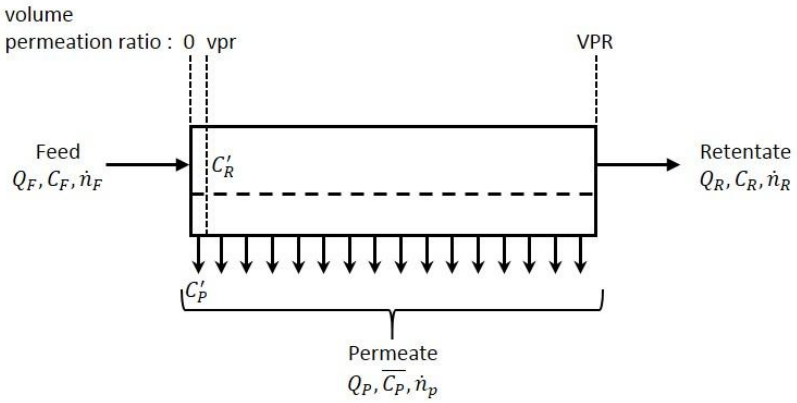

Figure A.1: Nanofiltration module divided into small elements

Eq. A.9 has to be integrated from the feed concentration to the retentate concentration and from 0 to VPR.

$$\int_{C_F}^{C_R} \frac{\mathrm{d}C_R'}{C_R'} = -\int_0^{VPR} \frac{R \times \mathrm{d}(1 - vpr)}{1 - vpr} \tag{A.10}$$

After integration, one gets:

$$\ln(C_R) - \ln(C_F) = -R \times [\ln(1 - VPR) - \ln(1)] \tag{A.11}$$

Eq. A.11 can be rewritten to get Eq. A.12.

$$C_R = C_F \times (1 - VPR)^{-R} \tag{A.12}$$

Replacing VPR by VRR leads to:

$$C_R = C_F \times VRR^R \tag{A.13}$$

The concentration can be transposed to the molar flowrate.

$$\dot{n}_R = \dot{n}_F \times \frac{Q_R}{Q_F} \times VRR^R \tag{A.14}$$

Combining Eq. A.14 and Eq. 2 leads to the final equation.

$$\dot{n}_R = \dot{n}_F \times VRR^{(R-1)} \tag{A.15}$$

References

[1] D. Nair, J.T. Scarpello, L.S. White, L.M. Freitas dos Santos, I.F.J. Vankelecom, A.G. Livingston, Semi-continuous nanofiltration-coupled Heck reactions as a new approach to improve productivity of homogeneous catalysts, Tetrahedron Lett. 42 (2001) 8219–8222. doi:10.1016/S0040-4039(01)01734-8.

[2] A. Datta, K. Ebert, H. Plenio, Nanofiltration for Homogeneous Catalysis Separation: Soluble

Polymer-Supported Palladium Catalysts for Heck, Sonogashira, and Suzuki Coupling of Aryl Halides, Organometallics 22 (2003) 4685–4691. doi:10.1021/om0303754.

[3] S. Aerts, A. Buekenhoudt, H. Weyten, L.E.M. Gevers, I.F.J. Vankelecom, P.A. Jacobs, The use of solvent resistant nanofiltration in the recycling of the Co-Jacobsen catalyst in the hydrolytic kinetic resolution (HKR) of epoxides, J. Membr. Sci. 280 (2006) 245–252. doi:10.1016/j.memsci.2006.01.025.

[4] A. Keraani, T. Renouard, C. Fischmeister, C. Bruneau, M. Rabiller-Baudry, Recovery of enlarged olefin metathesis catalysts by nanofiltration in an eco-friendly solvent, ChemSusChem. 1 (2008) 927–933. doi:10.1002/cssc.200800152.

[5] L. Peeva, J. Arbour, A. Livingston, On the Potential of Organic Solvent Nanofiltration in Continuous Heck Coupling Reactions, Org. Process Res. Dev. 17 (2013) 967–975. doi:10.1021/op400073p.

[6] M. Rabiller-Baudry, G. Nasser, T. Renouard, D. Delaunay, M. Camus, Comparison of two nanofiltration membrane reactors for a model reaction of olefin metathesis achieved in toluene, Sep. Purif. Technol. 116 (2013) 46–60. doi:10.1016/j.seppur.2013.04.052.

[7] J. Guerra, D. Cantillo, C.O. Kappe, Visible-light photoredox catalysis using a macromolecular ruthenium complex: reactivity and recovery by size-exclusion nanofiltration in continuous flow, Catal. Sci. Technol. 6 (2016) 4695–4699. doi:10.1039/C6CY00070C.

[8] J. Dreimann, P. Lutze, M. Zagajewski, A. Behr, A. Górak, A.J. Vorholt, Highly integrated reactor–separator systems for the recycling of homogeneous catalysts, Chem. Eng. Process. Process Intensif. 99 (2016) 124–131. doi:10.1016/j.cep.2015.07.019.

[9] S. Darvishmanesh, L. Firoozpour, J. Vanneste, P. Luis, J. Degrève, B. Van der Bruggen, Performance of solvent resistant nanofiltration membranes for purification of residual solvent in the pharmaceutical industry: experiments and simulation, Green Chem. 13 (2011) 3476–3483. doi:10.1039/C1GC15462A.

[10] J. Vanneste, D. Ormerod, G. Theys, D. Van Gool, B. Van Camp, S. Darvishmanesh, B. Van der Bruggen, Towards high resolution membrane-based pharmaceutical separations, J. Chem. Technol. Biotechnol. 88 (2013) 98–108. doi:10.1002/jctb.3848.

[11] L.S. White, A.R. Nitsch, Solvent recovery from lube oil filtrates with a polyimide membrane, J. Membr. Sci. 179 (2000) 267–274. doi:10.1016/S0376-7388(00)00517-2.

[12] V.S.K. Adi, M. Cook, L.G. Peeva, A.G. Livingston, B. Chachuat, Optimization of OSN Membrane Cascades for Separating Organic Mixtures, in: Z.K. and M. Bogataj (Ed.), Comput. Aided Chem. Eng., Elsevier, Amsterdam, Netherlands, 2016: pp. 379–384. doi.org/10.1016/B978-0-444-63428-3.50068-0

[13] P. Vandezande, L.E.M. Gevers, I.F.J. Vankelecom, Solvent resistant nanofiltration: separating on a molecular level, Chem. Soc. Rev. 37 (2008) 365–405. doi:10.1039/b610848m.

[14] P. Marchetti, M.F. Jimenez Solomon, G. Szekely, A.G. Livingston, Molecular Separation with Organic Solvent Nanofiltration: A Critical Review, Chem. Rev. 114 (2014) 10735–10806. doi:10.1021/cr500006j.

[15] G. Szekely, M.F. Jimenez-Solomon, P. Marchetti, J.F. Kim, A.G. Livingston, Sustainability assessment of organic solvent nanofiltration: from fabrication to application, Green Chem. 16 (2014) 4440–4473. doi:10.1039/C4GC00701H.

[16] A. Caus, L. Braeken, K. Boussu, B. Van der Bruggen, The use of integrated countercurrent nanofiltration cascades for advanced separations, J. Chem. Technol. Biotechnol. 84 (2009) 391–398. doi:10.1002/jctb.2052.

[17] J.C.-T. Lin, A.G. Livingston, Nanofiltration membrane cascade for continuous solvent exchange, Chem. Eng. Sci. 62 (2007) 2728–2736. doi:10.1016/j.ces.2006.08.004.

[18] W.E. Siew, A.G. Livingston, C. Ates, A. Merschaert, Molecular separation with an organic solvent nanofiltration cascade – augmenting membrane selectivity with process engineering, Chem. Eng. Sci. 90 (2013) 299–310. doi:10.1016/j.ces.2012.10.028.

[19] R. Abejón, A. Garea, A. Irabien, Analysis and optimization of continuous organic solvent nanofiltration by membrane cascade for pharmaceutical separation, AIChE J. 60 (2014) 931–948. doi:10.1002/aic.14345.

[20] P. Schmidt, E.L. Bednarz, P. Lutze, A. Górak, Characterisation of Organic Solvent Nanofiltration membranes in multi-component mixtures: Process design workflow for utilizing targeted solvent modifications, Chem. Eng. Sci. 115 (2014) 115-126. doi:10.1016/j.ces.2014.03.029.

[21] M. Priske, K.D. Wiese, A. Drews, M. Kraume, G. Baumgarten, Reaction integrated separation of homogenous catalysts in the hydroformylation of higher olefins by means of organophilic nanofiltration, J. Membr. Sci. 360 (2010) 77–83. doi:10.1016/j.memsci.2010.05.002.

[22] R. Abejón, A. Garea, A. Irabien, Optimum design of reverse osmosis systems for hydrogen peroxide ultrapurification, AIChE J. 58 (2012) 3718–3730. doi:10.1002/aic.13763.

[23] M.S. Avgidou, S.P. Kaldis, G.P. Sakellaropoulos, Membrane cascade schemes for the separation of LPG olefins and paraffins, J. Membr. Sci. 233 (2004) 21–37. doi:10.1016/j.memsci.2003.12.007.

[24] G. Al-Enezi, N. Fawzi, Design consideration of RO units: Case studies, Desalination. 153 (2003) 281–286. doi:10.1016/S0011-9164(02)01147-5.

[25] W.E. Siew, A.G. Livingston, C. Ates, A. Merschaert, Continuous solute fractionation with membrane cascades – A high productivity alternative to diafiltration, Sep. Purif. Technol. 102 (2013)

1–14. doi:10.1016/j.seppur.2012.09.017.

[26] B. Van der Bruggen, M. Mänttäri, M. Nyström, Drawbacks of applying nanofiltration and how to avoid them: A review, Sep. Purif. Technol. 63 (2008) 251–263. doi:10.1016/j.seppur.2008.05.010.

[27] L. Peeva, J. Da Silva. Burgal, I. Valtcheva, A.G. Livingston, Continuous purification of active pharmaceutical ingredients using multistage organic solvent nanofiltration membrane cascade, Chem. Eng. Sci. 116 (2014) 183–194. doi:10.1016/j.ces.2014.04.022.

[28] A. Caus, S. Vanderhaegen, L. Braeken, B. Van der Bruggen, Integrated nanofiltration cascades with low salt rejection for complete removal of pesticides in drinking water production, Desalination. 241 (2009) 111–117. doi:10.1016/j.desal.2008.01.061.

[29] A. Lejeune, M. Rabiller-Baudry, T. Renouard, B. Balannec, Y. Liu, J. Augello, D. Wolbert, An original graphical tool easy to handle for decision making to design cascade of membranes of organic solvent nanofiltration for homogeneous catalyzed reactions, submitted to Chem. Eng. Sci. (Under revision).

Highlights

Flexible architecture and original equations used for the simulation of cascades.

75 cascade configurations systematically studied and developed with VRR from 2 to 10.

Graphical representation to select the best configuration based on specific criteria.

A careful attention should be paid to all parameters to ensure realistic proposals.

Graphical abstract